MEASUREMENTS OF ROCK CORE DISPERSIVITY AND TORTUOSITY FOR MULTI-PHASE SYSTEMS

Marco Zecca[a], Abdolvahab Honari[a], Sarah J. Vogt[a], Branko Bijeljic[b], Eric F. May[a] and Michael L. Johns[a]
[a] School of Mechanical and Chemical Engineering M050, University of Western Australia, 35 Stirling Highway, Crawley 6009, Western Australia, Australia.
[b] Department of Earth Science and Engineering, Imperial College London, Prince Consort Road, London SW7 2BP, United Kingdom.

This paper was prepared for presentation at the International Symposium of the Society of Core Analysts held in Snowmass, Colorado, USA, 21-26 August 2016

ABSTRACT
Known as CSEGR (Carbon Sequestration with Enhanced Gas Recovery), sequestered CO_2 can be used to re-pressurise partially depleted natural gas reservoirs to increase gas recovery, with the intention to also store the CO_2. Because natural gas and CO_2 are fully miscible, simulations require CO_2-natural gas dispersion at supercritical conditions to be accurately measured in order to quantify this mixing and hence establish the viability of CSEGR. We have designed and constructed a unique core flooding apparatus capable of accurately determining such supercritical gas dispersivity; this has been measured in two sandstones and two carbonates cores as a function of temperature, pressure and interstitial velocity. This is supplemented with Nuclear Magnetic Resonance (NMR) measurements of tortuosity to quantify the underpinning effective diffusion process. The resultant dispersivity data (K - Peclet number (Pe) plot) and tortuosity data are combined and presented in a format which is readily incorporated into CSEGR simulations.

INTRODUCTION
Even though enhanced oil recovery (EOR) via CO_2 flooding is a promising method to improve the recovery factor of oil reservoirs and geologically sequester CO_2, enhanced gas recovery (EGR) with CO_2 flooding/sequestration has not been widely considered by the oil and gas industry. The only current field-scale EGR project is the Rotliegend K12-B gas reservoir, located offshore of the Netherlands, which started in 2004 after 17 years of conventional gas production (Vandeweijer *et al.*, 2011). A Canadian depleted gas reservoir was also used for an EGR/CO_2 sequestration trial in 2002 but the operation was terminated after three years due to the early CO_2 breakthrough into the producing wells (Pooladi-Darvish et al., 2008).

EGR cannot only safely store CO_2 within the formation but also can improve the natural gas recovery by maintaining the reservoir pressure and enhancing sweep efficiency and production rates. However, natural gas and CO_2 are entirely miscible in all proportions and consequently the risks of extensive mixing of these fluids within the reservoir formation and early CO_2 breakthrough into production wells are the main hurdles for EGR implementation. These associated risks and uncertainties of EGR projects can be estimated by using reservoir simulations in which fluid flow in reservoir formations can be quantitatively modeled and, in principle, the mixing process between the injected CO_2 and natural gas captured. Doing so reliably, however, requires (1) adequate characterization of physical dispersion at all relevant length-scales, and (2) that numerical dispersion in such simulations be kept sufficiently small. Extensive studies of dispersion at the field scale have been published (Arya et al., 1988; Coats et al., 2009a; Lake, 1989) but generalizing the results of these studies is not straightforward. Physical dispersion at smaller length scales is also important because the description of transport at the core scale can play an important role in the prediction of mixing at the field scale.

In this work, a unique core flooding apparatus capable of accurately determining supercritical gas dispersivity has been designed and constructed. The measured dispersion coefficients (K_L) of CO_2 and CH_4 for two sandstone cores (Berea and Donnybrook) and two carbonate rock samples (Ketton and Estaillades) are presented over a range of pressure, temperature, and interstitial velocities. These highly reproducible data are used to obtain the characteristic mixing length-scale for the different rocks. These measurements were extended to also consider the effect of residual water on the dispersion process and were supplemented by an independent measurement of tortuosity using appropriate NMR methodology.

THEORY

Dispersion in floods of cylindrical core plugs with injection along the axis can be adequately described by the one-dimensional advective-dispersion (AD) equation:

$$\frac{\partial C}{\partial t} = K_L \frac{\partial^2 C}{\partial x^2} - u_m \frac{\partial C}{\partial x} \quad , \qquad (1)$$

where C is the concentration of the dispersing species, t is time, K_L is the longitudinal dispersion coefficient and u_m is the mean interstitial velocity in the direction of bulk flow, x, in the porous medium. We note the use of alternative models (continuous time random walks and multi-rate mass transfer models) to describe dispersion in more complex, heterogeneous porous media (e.g. Haggerty and Gorelick, 1995; Berkowitz et al., 2006). The ratio of the dispersion coefficient calculated from Eq. (1) to the diffusion coefficient, K_L/D, has been commonly plotted as a function of Peclet number. This is defined here as $\alpha u_m/D$ where α denotes the medium dispersivity. This differs from the classical definition in which grain/particle diameter replaces α as the characteristic length scale for mixing in the pores (Perkins and Johnston, 1963). Note that this latter definition is inappropriate for consolidated media such as the rock cores studied here.

Additionally, Eq.**(2)** has been frequently used to characterize the different dispersion behaviors evident in such correlated data:

$$\frac{K_L}{D} = \frac{1}{\tau} + \frac{\alpha u_m^n}{D}, \quad (2)$$

where τ is tortuosity, and *n* is an exponent. These three parameters characterize a given porous medium: generally $1 \leq n < 1.5$ (Brigham *et al.*, 1961; Gist et al., 1990; Legatski and Katz, 1967) and τ can range from $\sqrt{2}$ (for ideal packed beds only) to as much as 13 for certain consolidated media (Gist et al., 1990; Hurlimann et al., 1994). Generally for consolidated media these three parameters are treated empirically and must be determined from experiments with the rock; while τ can be determined via several methods, α and n can only be determined from core flooding experiments.

METHODOLOGY

Materials

The methane, carbon dioxide and nitrogen used in our experiments were supplied by BOC Scientific at purities greater than 0.999 mole fraction. Mixtures of CO_2 and CH_4 for pulse injection were prepared gravimetrically. Two types of 1.5 inch diameter sandstone cores, Berea and Donnybrook, and two carbonates, Estillades and Ketton were available. These cores were cleaned prior to use by Soxhlet extraction with a mole fraction mixture of 0.9 dicholormethane (Chem-Supply) + 0.1 methanol (Ajax-Finechem). The geometrical properties of the four cores used are listed in Table 1 with porosities, *Φ*, and permeabilities, *k*.

Core	Length (mm)	Diameter (mm)	$p_{confining}$ (MPa)	*Φ*	*k* (mD)
Berea sandstone	100.4	37.6	8	0.2043	463.3
			10	0.2039	460.7
			12	0.2036	458.2
Donnybrook sandstone	101	37.5	8	0.1576	12.07
			10	0.1573	12.01
			12	0.1572	11.95
Ketton carbonate	104.7	38.0	8	0.2277	2922.4
			10	0.2274	2912.2
			12	0.2270	2902.7
Estillades carbonate	105.6	37.9	8	0.2817	211.7
			10	0.0811	211
			12	0.2806	210.1

Table 1 Rock cores properties.

Apparatus and method

The specialized core flooding apparatus for $^{SC}CO_2$-CH_4 dispersion measurements was adapted from our previous experimental set-up for breakthrough measurements (Hughes *et al.*, 2012) to allow for pulse injection and to enable water delivery to, and drainage of, the rock core. A schematic of the apparatus is shown in Figure 1. A HPLC switching valve was included to allow for a controlled injection of a pulse of a 50% CH_4 and 50% CO_2 mixture. This composition was calculated as the best trade-off between minimizing density and viscosity contrasts between the fluids and maintaining an adequate signal to noise ratio. Analysis of the core effluent was conducted at measurement pressure using a HPIR cell and a syringe pump was used for effluent collection, ensuring better pressure regulation during the pulse displacement process. Details of the core holder, core wrapping, the core holder bath temperature control, pressure instrumentation and calibration of FT-IR spectrometer are included in our previous work (Hughes *et al.*, 2012). All experiments described below were conducted with the core in a vertical orientation.

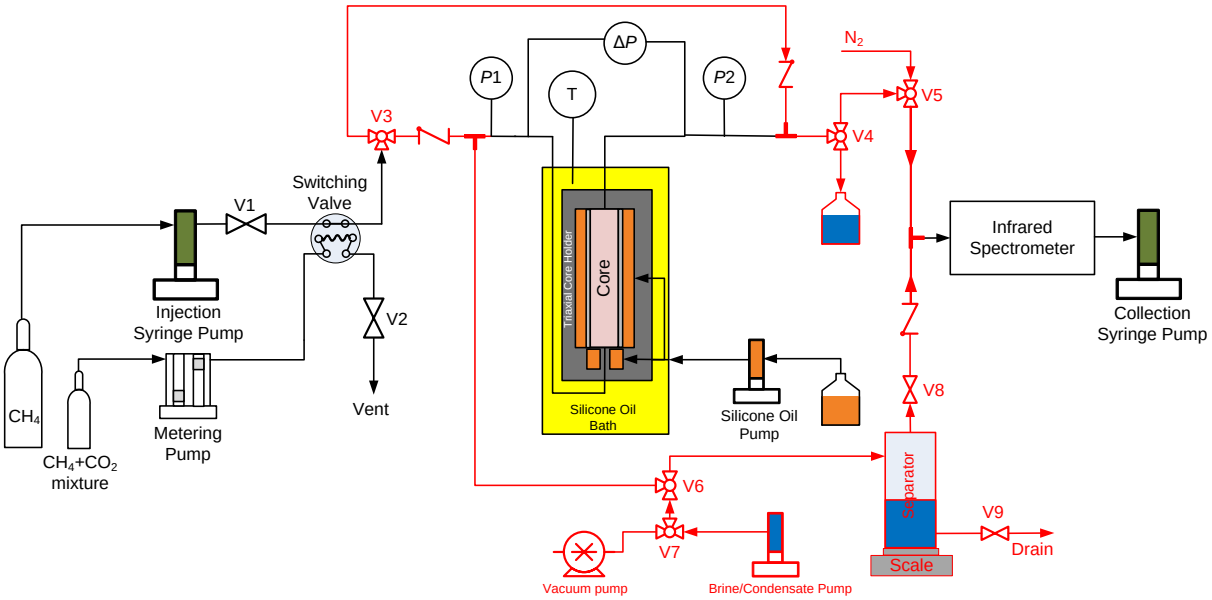

Figure 1 Simplified schematic of the core-flood apparatus for accurate dispersion measurements. The HPLC switching valve is shown in the sample loop filling position. To inject the pulse the valve is switched (rotated 180◦) so that the CH_4 flow flushes the sample out of the loop.

The flow from the injection pump was stopped when the dispersed pulse had passed completely through the IR cell. The experiments were conducted at core temperatures and pressures of 40 to 100 °C and 8 to 14 MPa, respectively, and with interstitial velocities between 0.004 and 1.908 $mm \cdot s^{-1}$.

Data analysis

For pulse experiments, the boundary conditions are:
$C(x > 0, t = 0) = 0$, $C(x = \infty, t) = 0$, $C(x = 0, 0 < t < \delta) = C_0$ and $C(x = 0, t > \delta) = 0$ where δ is the pulse duration. The solution to Eq. (1) with these boundary conditions (Levenspiel, 1999) is:

$$C = \frac{u_m}{\sqrt{4\pi K_L t}} \exp\left(-\frac{\left(L - u_m t\right)^2}{4K_L t} \right), \quad (3)$$

where L is the experimental length scale (core length). Eq.**(1)**, and its solution (Eq.**(3)**) are one–dimensional, as such they are unable to account for any velocity variations in the radial or cross-sectional direction.

However, Eq.**(3)** alone was not adequate for description of the effluent tracer concentration curves produced from the Ketton carbonate because of the non-Fickian/preasymptotic transport behavior associated with its heterogeneity in pore sizes. To describe this non-Fickian flow regime, several alternative models have been developed including the mobile-immobile model (MIM) (Deans (1963)), diffusion models, MRMT models (Haggerty and Gorelick, 1995) and CTRW models (Berkowitz *et al.*, 2006). In this case, it was found that the non-Fickian behavior of Ketton carbonate could be adequately modeled utilizing the MIM approach, which assumes the existence of two distinct regions in the rock, mobile and stagnant/immobile, and which describes the diffusional transport of species between these two zones using a first order mass transfer expression. This model was initially proposed by Deans (1963), who added two new parameters to Eq.**(1)**, namely the mass transfer coefficient and immobile volume fraction, but did not include the longitudinal dispersion coefficient. Coats and Smith (1964) modified Deans' version of Eq.**(1)** by adding this dispersion coefficient to produce (Coats and Smith, 1964; Van Genuchten and Wierenga, 1976)

$$\theta_m \frac{\partial C_m}{\partial t} + \theta_{im} \frac{\partial C_{im}}{\partial t} = \theta_m K_L \frac{\partial^2 C_m}{\partial x^2} \quad u_m \theta_m \frac{\partial C_m}{\partial x}, \quad (4)$$

$$\theta_{im} \frac{\partial C_{im}}{\partial t} = \beta\left(C_m - C_{im}\right) \quad (5)$$

where C_m and C_{im} are the concentrations of the dispersing solute species in the mobile and immobile regions, respectively; θ_m and θ_{im} are the mobile and stagnant fractions of the fluid in the porous media; β is a mass transfer coefficient; and u_m is the mean interstitial velocity in the mobile zone. To apply this solution to the measured effluent pulse profiles obtained for the Ketton core, the dispersion coefficient (K_L), the mobile fluid fraction (θ_m) and the mass transfer coefficient (β) were treated as the fitting parameters and the measured pulse breakthrough profiles were regressed to the analytical solutions of Eq. **(4)** and Eq.**(5)**.

The dispersion that occurs in the tubing leading to and from the core, and the inhomogeneous velocity profiles around the core entry and exit, both add to mixing and erroneously increase the apparent dispersion. As discussed in our previous work (Hughes *et al.*, 2012), to remove these effects measurements were conducted at the same conditions of T, P and flow rate with short and long Berea rock cores. The concentration profiles collected with the short core were used as inlet boundary conditions to a hypothetical undisturbed core of a length equal to the difference in length between our long and short core. Eq.**(1)** was solved numerically using a central finite difference method (the method of lines) implemented in Matlab within this hypothetical core and regressed to the experimental (long core) data in order to determine K_{corr}. In this manner this systematic error, between K_{long} extracted via Eq.**(3)** and the above methodology employing long and short core, was quantified. The modified setup produced a correction which was significantly dependent on velocity; a clear trend is shown in Figure 2. Consequently all K_{long} data measured for all the rock cores were corrected to account for these systematic errors as shown in Figure 2 to give the K_{corr} values listed in Table 2.

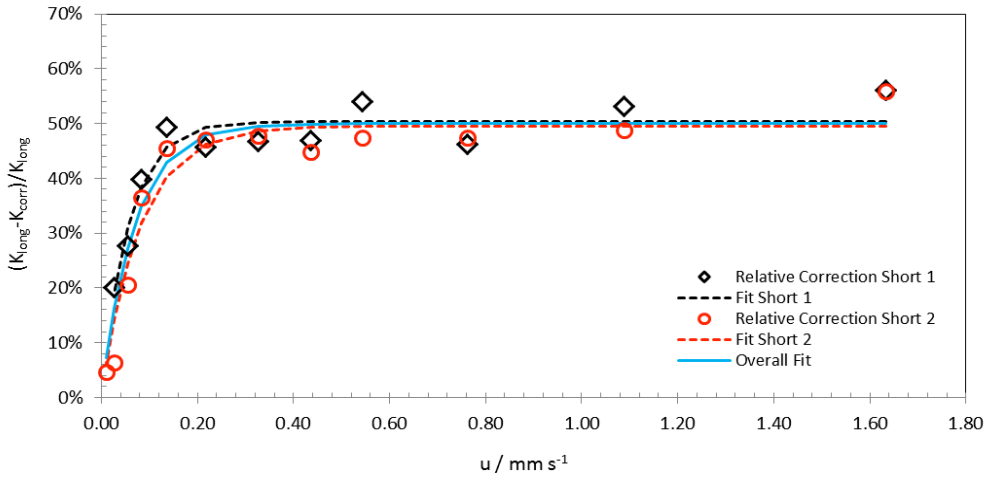

Figure 2 Relative size of dispersion coefficient correction as function of the interstitial velocity. The two data sets correspond to the two halves obtained from the cut of the original long core.

Independent measure of tortuosity

The diffusion coefficients D in Eq.**(2)**, which depend on pressure, temperature and composition, were obtained from the data of Takahashi and Iwasaki (1970). An error in the calculation of D would cause an offset in the value of (K_L/D) determined from the dispersion measurements, which would be most pronounced in the limit $u_m \rightarrow 0$. To confirm that no such offset was present, we measured the core's tortuosity, τ, using a second, completely independent technique. The Berea and Donnybrook rock core samples were evacuated and then saturated with distilled water at a pressure of 10 MPa and left for several hours to ensure complete saturation. These saturated cores were then placed in a 12.9 MHz nuclear magnetic resonance (NMR) rock core analyzer (Oxford Instruments) to

enable self-diffusion measurements via the application of pulsed field gradient stimulated-echo (PGSTE) techniques (Stejskal and Tanner, 1965). Measurement of the water's self-diffusion coefficient for a free liquid sample (D_0) and for the water in the saturated rock core (D), enables calculation of the system tortuosity ($\tau = D_0/D$) if a sufficiently long observation time is allowed to ensure the diffusion within the core is completely restricted. The same experiments were also run with methane at 3MPa providing a tortuosity consistent with the value obtained from water. In future, tortuosity will be measured as a function of the residual water content; D_2O will be adopted to avoid NMR signal from this wetting phase.

RESULTS AND DISCUSSION

'Dry' Sandstones and Carbonates

Table 2 summarizes all our experimental conditions (T, P and u_m), and a selection of dispersion coefficients (K_{corr}) for all the cores considered. The values of K_{corr} have been corrected for entry/exit and tubing effects as outlined above.

Core	T (°C)	P (MPa)	u (mm s^{-1})	D (10^{-8} m^2 s^{-1})	K_{corr} (10^{-8} m^2 s^{-1})
Berea	40	8	0.025	16.4	6.63
	40	8	0.499	16.4	22.12
	40	10	0.006	12.5	3.98
	40	10	0.140	12.5	9.58
	40	12	0.010	10.0	4.00
	40	12	0.199	10.0	10.37
	60	8	0.452	19.6	20.24
	60	10	0.012	15.2	5.39
	60	10	0.304	15.2	13.63
	60	12	0.004	12.3	3.21
	60	12	0.035	12.3	5.36
	80	8	0.034	23.1	8.00
	80	8	0.216	23.1	13.27
	80	10	0.016	18.0	6.18
	80	10	0.085	18.0	8.47
	80	12	0.120	14.7	8.45
	80	12	0.482	14.7	18.67
	100	8	0.085	26.6	10.17
	100	10	0.085	21.0	8.45
	100	10	0.142	21.0	9.64
	100	12	0.085	17.2	7.81
	100	12	0.207	17.2	10.18
Donnybrook	40	8	0.025	16.4	7.21
	40	8	0.140	16.4	18.22
	40	12	0.050	10.0	6.69
	40	12	0.141	10.0	18.66

	60	10	0.007	15.2	5.17
	60	10	0.304	15.2	39.95
	60	12	0.008	12.3	2.72
	60	12	0.035	12.3	5.36
Estillades	40	8	0.09	16.4	10.38
	40	10	0.004	12.5	3.79
	40	10	0.04	12.5	5.76
	40	12	1.151	10	140.03
	60	10	0.23	15.2	21.59
	60	10	1.149	15.2	133.65
	60	12	0.016	12.3	4.39
	60	12	1.646	12.3	214.59
Ketton	40	8	0.053	16.4	17.08
	40	10	0.011	12.5	8.49
	40	10	0.141	12.5	27.06
	40	10	1.124	12.5	212.49
	40	12	1.743	10	381.7
	40	14	1.908	8.1	424.03
	60	10	0.015	15.2	10.03
	60	10	0.745	15.2	115.94

Table 2 Dispersion coefficients of equimolar mixtures of CO_2–CH_4 into pure CH_4 or pure CO_2 for Berea, Donnybrook, Estillades and Ketton cores.

Application of Eq.**(2)** allowed the dispersivity (α) to be determined for the two sandstone cores. For the Berea and Donnybrook rocks, α = 0.35 mm and 1.31 mm, respectively, with a relative statistical uncertainty in these parameters from the regression of less than 5%. These values are consistent with those reported for sandstones by Coats *et al.* (2009b), although in the case of the Berea sandstone, the dispersivity measured here is moderately lower than other values reported in the literature (1.2 mm (Gist et al. (1990)); 3.75 mm (Brigham et al. (1961)); 2.2 mm (Legatski and Katz (1967)); 1-6 mm (Schulze-Makuch (2005))). However, as demonstrated by the discussions above, the value of the apparent dispersivity obtained can readily be affected by systematic measurement errors, compounded by the effects on α due to variation in sample length employed and, of course, variability in the actual samples used.

In Figure 3 the pulse breakthrough profiles of Estillades and Ketton carbonates show the reproducibility of the data and the better fitting obtained for Ketton with the MIM model in comparison to the AD equation.

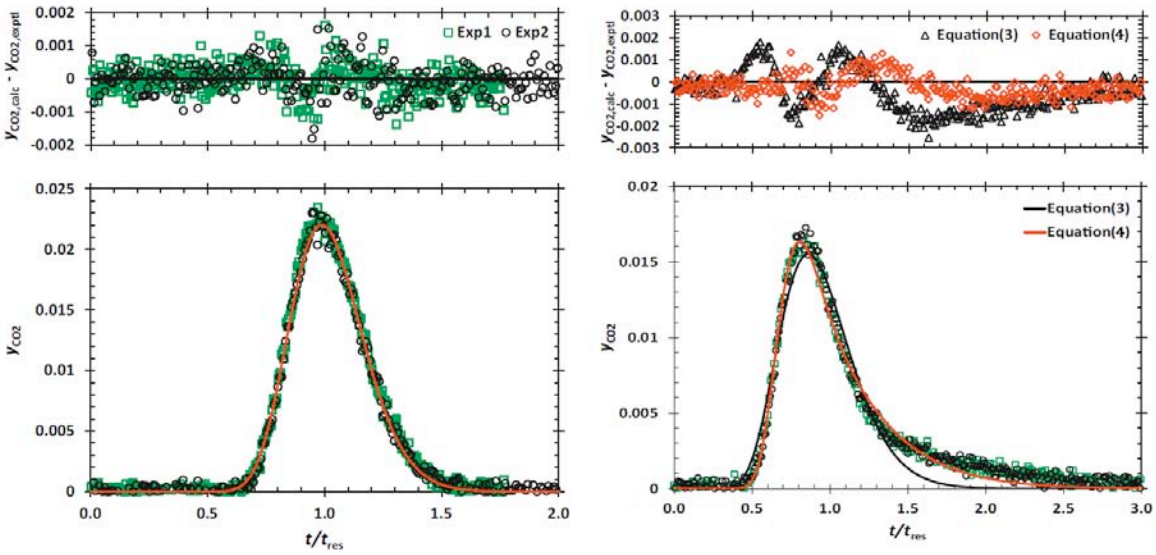

Figure 3 Left: repeatability of the pulse-breakthrough profiles for Estaillades carbonate core at 60°C, 10 MPa and 0.14 mm s^{-1}. Right: Ketton carbonate core at 60°C, 10 MPa and 0.28 mm s^{-1}. The lower panel demonstrates the breakthrough profiles and the fits achieved using Eq. (3) for Estaillades and both Eqs. (3) and (4) for Ketton. The upper panel shows the resulting residuals of the fits.

Our previous results showed the 1D-AD equation was adequate for the description of dispersion of CO_2-CH_4 system through sandstone cores. Larger dispersion coefficients at similar conditions for Donnybrook sandstone were reported, indicating a higher level of heterogeneity relative to the homogenous Berea sandstone. Because carbonate rocks are known as heterogeneous porous media, long tailing and early breakthrough profiles of the CO_2 together with comparatively higher dispersion coefficients were expected. After comparing several measured dispersion coefficients of the sandstones and carbonates at similar conditions, the dispersion coefficients for both carbonate samples were found to be larger than those for the homogeneous sandstone rock (Berea) whereas Estaillades showed similar dispersive behaviour to the more heterogeneous (Donnybrook) sandstone. Ketton exhibited the greatest dispersion among all the core samples used during this study. The pulse breakthrough profiles we observed for Ketton carbonate showed a more persistent long tail and an earlier breakthrough than for Estaillades carbonate.

The calculated dispersivities were then used to produce Figure 4 where the ratios of dispersion and diffusion coefficients, K_{corr}/D, were plotted against Pe_m. Also shown are two curves utilizing Eq.**(2)** where n was 1 for $Pe_m<1$ and 1.2 and 1.4 (power-law scaling) for $Pe_m>1$ (Bijeljic and Blunt, 2006; Bijeljic *et al.*, 2011). Figure 4 explicitly shows that the curves produced using Eq.**(2)** with n = 1.2 for sandstones and n = 1.4 for carbonates are an excellent fit with the Donnybrook and Ketton data respectively for $Pe_m>10$. This provides experimental validation for the power law exponents derived from transport simulations (e.g. Bijeljic and Blunt (2006) and Bijeljic et al. (2011)). Finally, the $Pe_m<100$ considered in the study is lower compared to other standard curves reported in literature

(e.g. Seymour and Callaghan (1997)) since this the IR spectrometer could not detect the breakthrough pulse for higher velocities due to the limited time resolutions of the instrument.

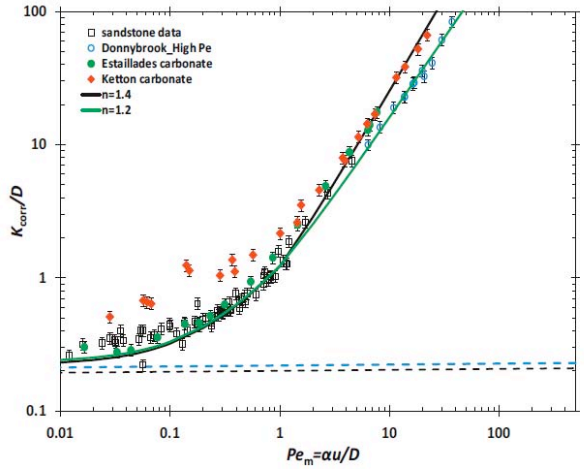

Figure 4 Measured K_{corr}/D vs. Pe_m for Berea and Donnybrook sandstone and Ketton and Estaillades carbonate cores. The dashed lines indicate the independent NMR measurements of sandstone rocks tortuosity. The fitted curves are produced by Eq. (2) for n equal to 1.2 and 1.4.

Inclusion of Residual Water

Figure 5 shows the impact of connate or residual water on the breakthrough profiles for Donnybrook. The presence of this second phase clearly increases the dispersion significantly, the corresponding dispersion coefficients are 5.7×10^{-7} and 39.0×10^{-7} $m^2\cdot s^{-1}$ respectively. Future work will quantitatively measure the dependence of medium properties such as dispersivity on the residual water content.

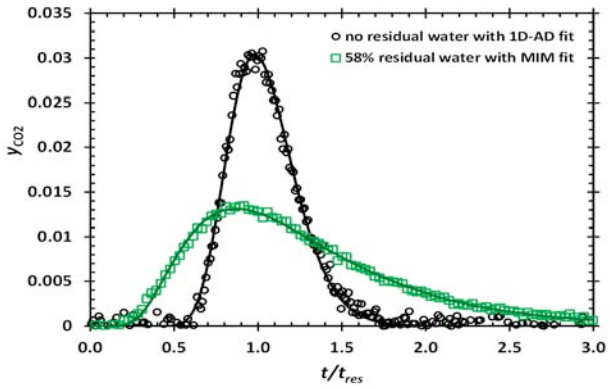

Figure 5 Pulse breakthrough profiles obtained for Donnybrook dry and 58% saturated with water. The measurements were made at 40 °C, 10 MPa and with an interstitial velocities 0.34 $mm\cdot s^{-1}$.

Measurement of Tortuosity

The NMR measurements of tortuosity (τ), using water with diffusion times between 10ms and 1s, were 4.3 and 4.8 for Berea and Donnybrook sandstone cores, respectively. In literature, lower values of tortuosities have been reported from electrical measurements (Zhan et al. (2011)). The tortuosity value for the Berea rock core was also calculated by measuring the self-diffusion coefficient of methane at 3MPa; the tortuosity value in this case was 4.5 which is broadly in agreement with the water measurement. In Figure 6 we show the raw signal attenuation NMR data – the slope of these data provides the diffusion coefficient according to the Stejskal-Tanner equation (Stejskal and Tanner, 1965) and the ratio of the free to restricted diffusion coefficient provides the tortuosity, τ. The diffusion time for these measurements was 100 ms, ensuring the diffusion to be fully restricted ((Hurlimann (1994). In future we will measure τ as a function of water content.

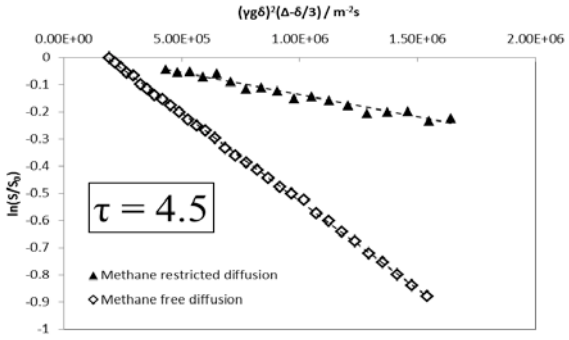

Figure 6 NMR diffusion measurements of free and restricted methane at 3MPa.

CONCLUSIONS

A pulsed measurement apparatus was established for the measurement of the dispersion coefficient (*K*) for $^{SC}CO_2$ and CH_4 and successfully applied to two sandstones and two carbonates samples. The methodology was adapted to minimize the effects of density and concentration contrasts; the reproducibility obtained were excellent. By using 1D- ADE approach for sandstones and Estillades carbonate and a mobile-immobile model to analyse the breakthrough profiles observed for the Ketton carbonate, asymptotic dispersion coefficients were obtained and compared. All acquired data collapsed onto a common curve when K/D was plotted as a function of Pe_m, capturing variation with temperature and pressure. Preliminary results showed the impact of residual water on the dispersion mechanism and independent measurements of tortuosity with water and methane also produced consistent results.

ACKNOWLEDGEMENTS

This work was supported by the Western Australian Department of Environment and Conservation through the Low Emissions Energy Development fund.

REFERENCES

Arya, A., Hewett, T. A., Larson, R. G., Lake, L. W., 1988. Dispersion and reservoir heterogeneity SPE Reservoir Engineering 3, 139-148.

Berkowitz, B., Cortis, A., Dentz, M., Scher, H., 2006. Modeling non-fickian transport in geological formations as a continuous time random walk, Reviews of Geophysics 44, 1-49.

Bijeljic, B., Blunt, M. J., 2006. Pore-scale modeling and continuous time random walk analysis of dispersion in porous media, Water Resources Research 42, W01202.

Bijeljic, B., Mostaghimi, P., Blunt, M. J., 2011. Signature of non-Fickian solute transport in complex heterogeneous porous media, Physical Review Letters 107, 204502.

Brigham, W. E., Reed, P. W., Dew, J. N., 1961. Experiments on mixing during miscible displacement in porous media, SPE Journal 1, 1-8.

Coats, K. H., Smith, B. D., 1964. Dead-end pore volume and dispersion in porous media, SPE Journal 4, 73-84.

Coats, K. H., Whitson, C. H., Thomas, L. K., 2009a. Modeling Conformance as Dispersion, SPE Reservoir Evaluation & Engineering 12, 33-47.

Coats, K. H., Whitson, C. H., Thomas, L. K., 2009b. Modeling conformance as dispersion, SPE Reservoir Evaluation & Engineering 12, 33-47.

Deans, H. A., 1963. A mathematical model for dispersion in the direction of flow in porous media Society of Petroleum Engineers Journal 3, 49-52.

Gist, G. A., Thompson, A. H., Katz, A. J., Higgins, R. L., 1990. Hydrodynamic dispersion and pore geometry in consolidated rock, Physics of Fluids A 2, 1533-1544.

Haggerty, R., Gorelick, S. M., 1995. Multiple-rate mass transfer for modeling diffusion and surface reactions in media with pore-scale heterogeneity, Water Resources Research 31, 2383-2400.

Hughes, T. J., Honari, A., Graham, B. F., Chauhan, A. S., Johns, M. L., May, E. F., 2012. CO_2 sequestration for enhanced gas recovery: new measurements of supercritical CO_2-CH_4 dispersion in porous media and a review of recent research, International Journal of Greenhouse Gas Control 9, 457-468.

Hurlimann, M. D., Helmer, K. G., Latour, L. L., Sotak, C. H., 1994. Restricted diffusion in sedimentary rocks. determination of surface-area-to-volume ratio and surface relaxivity, Journal of Magnetic Resounance, Series A 111, 169-178.

Lake, L. W., 1989. Enhanced oil recovery Prentice Hall 550, New Jersey, USA.

Legatski, M. W., Katz, D. L., 1967. Dispersion coefficients for gases flowing in consolidated porous media, SPE Journal 7, 43-53.

Levenspiel, O., 1999. Chemical reaction engineering 3rd ed. John Wiley & Sons.

Perkins, T. K., Johnston, O. C., 1963. A review of diffusion and dispersion in porous media, SPE Journal 3, 70-84.

Pooladi-Darvish, M., Hong, H., Theys, S., Stocker, R., Bachu, S., Dashtgard, S., 2008. CO_2 injection for enhanced gas recovery and geological storage of CO_2 in the long Coulee Glauconite F pool, Alberta. In SPE (Ed.), SPE Annual Technical Conference and Exhibition, Denver, Colorado.

Schulze-Makuch, D., 2005. Longitudinal dispersivity data and implications for scaling behavior, Ground Water 43, 443-456.

Seymour, J. D., Callaghan, P. T., 1997. Generalized Approach to NMR Analysis of Flow and Dispersion in Porous Media, AIChE Journal 43, 2096-2111.

Stejskal, E. O., Tanner, J. E., 1965. Spin diffusion measurements: spin echoes in the presence of a time dependent field gradient The Journal of Chemical Physics 42, 288-292.

Takahashi, S., Iwasaki, H., 1970. The diffusion of gases at high pressures. III. The diffusion of $^{14}CO_2$, in the $^{12}CO_2$-CH_4 system, Bulletin of the Chemical Research Institute of Non-Aqueous Solutions, Tohoku University 20, 27-36.

Van Genuchten, M. T., Wierenga, P. J., 1976. Mass transfer studies in sorbing porous media I. analytical solutions, Soil Science Society of America Journal 40, 473-480.

Vandeweijer, V., van der Meer, L. G. H., Hofstee, C., Mulders, F., Graven, H., D'Hoore, D., 2011. Monitoring CO_2 Injection at K12-B http://www.co2geonet.com/UserFiles/file/Open%20Forum%202011/PDF-presentations/2-10_Vanderweijer.pdf.

Zhan, X., Zhu, Z., ToksoZ, M. N., 2011. Quantitative DC and high frequency AC seismoelectric measurement on Berea sandstone, SEG Technical Program Expanded Abstracts 30, 2246-2250.